Comparative Immune Profiling of Murine and Human Pancreatic Cancer Precursors Reveals Species- and Lesion-Dependent Immune Microenvironments

Lena Haeberle-Graser, Marie Schulte, Carolin Mueller, Sebastian Haensch, Martin Schlensog, Irene Esposito

Article - Version of Record

Suggested Citation:
Häberle, L., Schulte, M., Müller, C., Hänsch, S., Schlensog, M., & Esposito, I. (2026). Comparative Immune Profiling of Murine and Human Pancreatic Cancer Precursors Reveals Species- and Lesion-Dependent Immune Microenvironments. Laboratory Investigation, 106(8), Article 106143. https://doi.org/10.1016/j.labinv.2026.106143

Lab Invest 106 (2026) 106143

LABORATORY INVESTIGATION

journal homepage: https://laboratoryinvestigation.org/

Research Article

Comparative Immune Profiling of Murine and Human Pancreatic Cancer Precursors Reveals Species- and Lesion-Dependent Immune Microenvironments

Lena Haeberle-Graser[a], Marie Schulte[a,b], Carolin Mueller[a,c], Sebastian Haensch[d], Martin Schlensog[a], Irene Esposito[a,*]

[a] *Institute of Pathology, Heinrich Heine University & University Hospital Duesseldorf, Germany;* [b] *Barmherzige Brueder Hospital Regensburg, Department of Anesthesiology and Surgical Intensive Care Medicine, Germany;* [c] *Department of Pediatrics, Helios Klinikum Krefeld, Academic Hospital RWTH Aachen, Germany;* [d] *Center for Advanced Imaging (CAi), Heinrich Heine University Duesseldorf, Germany*

ARTICLE INFO

Article history:
Received 19 July 2025
Revised 9 May 2026
Accepted 23 May 2026
Available online 3 June 2026

Keywords:
genetically engineered mouse models
immune microenvironment
intraductal papillary mucinous neoplasia
pancreatic ductal adenocarcinoma
pancreatic cancer precursors
tumor microenvironment

ABSTRACT

Purpose: This study aimed to comparatively characterize the immune microenvironment (iME) in murine and human precursor lesions of pancreatic ductal adenocarcinoma (PDAC) to better understand its role in pancreatic carcinogenesis.
Materials and Methods: Tissue microarrays were constructed from 41 transgenic mice (140 samples including normal pancreas tissue, acinar-ductal metaplasia [ADM], pancreatic intraepithelial neoplasms [PanIN], and PDAC) and from 76 patients (221 samples including normal pancreas tissue, ADM, PanIN, intraductal papillary mucinous neoplasms [IPMN], mucinous cystic neoplasms [MCN], and PDAC). OPAL7 multiplex immunofluorescence was used for simultaneous detection of multiple immune cell markers (CD3, CD4, CD8, CD8a, FoxP3, PD-1, CD19, CD20, F4/80, CD68, CD163, tryptase, and granzyme B), followed by software-assisted image-based quantification.
Results: The iME of all lesions was characterized by a predominance of $CD3^+$ T lymphocytes over B lymphocytes, except for murine PanIN, which showed $CD19^+$ B cell predominance. Both murine and human PDAC showed an immunosuppressive iME. However, precursor lesions differed markedly: murine ADM and PanIN showed no significant immune cell increases, while human ADM already displayed elevated mast cells, macrophages, T helper cells, and Tregs. Human ADM, PanIN, and gastric-type IPMN showed a significant increase in $CD8^+$ cytotoxic T cells compared with normal pancreas tissue, while cytotoxic T cells were decreased in PDAC. In contrast, human intestinal-type IPMN and MCN showed no increase in cytotoxic T cells.
Conclusions: These findings highlight that the iME evolves during pancreatic carcinogenesis and differs significantly between species and lesion types. The immune landscape of murine models does not fully recapitulate that of human disease, emphasizing the need for caution when translating preclinical findings. Moreover, distinct immune profiles across human precursor subtypes suggest precursor-specific mechanisms of immune engagement.

* Corresponding author.
E-mail address: Irene.Esposito@med.uni-duesseldorf.de (I. Esposito).

https://doi.org/10.1016/j.labinv.2026.106143

Introduction

Pancreatic cancer is an exceptionally lethal malignancy with limited curative therapy options.[1] Although the incorporation of immunotherapy into treatment regimens has undoubtedly led to a paradigm shift in the management of many other solid malignancies, the same cannot be said about the treatment of pancreatic cancer. Studies exploring immunotherapy for pancreatic ductal adenocarcinoma (PDAC) have largely shown discouraging results. In part, this is thought to be the result of the low mutational burden of PDAC compared with other solid malignancies such as lung cancer or malignant melanoma.[2] The comparatively low number of somatic mutations in PDAC leads to a low number of altered proteins produced by the tumor, so-called neoantigens, which allow for the immune system to recognize the tumor as foreign, triggering an immune response targeted against the tumor cells. Correspondingly, rare cases of long-term survivors of PDAC are characterized by a high number of tumor-specific high-quality neoantigens and, consequently, high numbers of antitumor cytotoxic T cells.[3] This is also consistent with the fact that monotherapy with an immune checkpoint inhibitor has shown beneficial effects in a very small subset of pancreatic cancer patients, that is, those with microsatellite instability (MSI; 1%-2%, occurring significantly more frequently in mucinous and medullary pancreatic cancer compared with conventional PDAC),[4,5] although the response to immunotherapy of MSI-high PDAC is still worse compared with that of most other MSI-high entities.[6]

However, it is known that the immunogenicity of tumors—or lack thereof—is not an invariable predetermined parameter but rather a dynamic process, which may undergo significant change during the course of the disease,[7] indicating that other factors than merely the tumor mutational burden must be at play. PDAC is generally characterized by an immunosuppressive and immunoevasive tumor microenvironment (TME).[8] Briefly, the TME of PDAC is composed of extracellular matrix (ECM) proteins, blood vessels, cancer-associated fibroblasts, pancreatic stellate cells, and various immune cells. The total population of tumor-associated immune cells is known as the immune microenvironment (iME). The iME can include generally immunoactive or immunosupportive cell types such as cytotoxic T cells on one hand, as well as immunosuppressive cell types such as tumor-associated macrophages, myeloid-derived suppressor cells, and regulatory T cells (Treg cells), on the other hand. Not surprisingly, studies have shown that immunosuppressive cell types are generally enriched in PDAC. Understanding when and how this immunosuppressive TME is initiated and promoted during pancreatic carcinogenesis is a pivotal first step in overcoming immunosuppression in pancreatic cancer and to possibly find ways to intervene in pancreatic carcinogenesis at the stage of precursor lesions.

Tenascin C (TNC) and periostin (POSTN) are (glyco-)proteins of the ECM, which have been shown to be overexpressed in PDAC[9-11] and are hypothesized to be involved in modulating the iME in various diseases. Briefly, TNC can exert immunoactive properties on one hand, for example, by upregulating genes involved in antigen processing and presenting but, on the other hand, can play an immunosuppressive role, for example, by forming of a physical barrier trapping tumor-infiltrating $CD8^+$ T cells.[12,13] POSTN is thought to exert mostly immunosuppressive functions, for example, its expression has been shown to be associated with increased M2 macrophage infiltration.[14]

A simultaneous analysis of murine and human tissues using cohorts of well-characterized PDAC precursors was conducted to achieve a comparative and detailed characterization of the iME of PDAC precursors in mice and humans. Genetically engineered mouse models of pancreatic cancer with genetic knockout of TNC and POSTN were used to investigate their effects on the iME.

Materials and methods

Collection of Murine Tissue and Preparation of Murine Tissue Microarrays

$Ptf1aCre^{tg/+}$;$LSL\text{-}Kras^{G12D/+}$ (KC; n = 7) and $Ptf1aCre^{tg/+}$;$LSL\text{-}Kras^{G12D/+}$;$p53^{flox/flox}$ or $Ptf1aCre^{tg/+}$;$LSL\text{-}Kras^{G12D/+}$;$p53^{flox/+}$ (KPC-like; n = 37) mice were used; 13 mice had an additional knockout of the ECM protein TNC ($Ptf1aCre^{tg/+}$;$LSL\text{-}Kras^{G12D/+}$;$p53^{flox/+}$;$TNC^{-/-}$ or $Ptf1aCre^{tg/+}$;$LSL\text{-}Kras^{G12D/+}$;$p53^{flox/flox}$;$TNC^{-/-}$), and 10 mice had an additional knockout of the ECM protein POSTN ($Ptf1aCre^{tg/+}$;$LSL\text{-}Kras^{G12D/+}$;$p53^{flox/flox}$;$POSTN^{-/-}$, $Ptf1aCre^{tg/+}$;$LSL\text{-}Kras^{G12D/+}$;$p53^{flox/+}$;$POSTN^{-/-}$ and $Ptf1aCre^{tg/+}$;$LSL\text{-}Kras^{G12D/+}$;$POSTN^{-/-}$) (Table 1).

Mice were sacrificed and organs harvested when the pancreas was markedly enlarged and/or the general condition worsened significantly (range, 37 days to 480 days from birth). An overview of the transgenic mouse cohort is given in Table 1.

In total, 140 tissue microarray (TMA) spots were created. Regions of interest from normal pancreatic tissue, pancreatic cancer precursors lesions (acinar-ductal metaplasia [ADM] and pancreatic intraepithelial neoplasia [PanIN]), invasive PDAC and their surrounding TME, respectively, were selected and transferred to 2 TMA blocks (Manual Tissue Arrayer MTA-1; AlphaMetrix Biotech). A 1-mm core size was used. An overview of all murine TMA samples is given in Table 1.

Collection of Human Tissue Samples and Preparation of Human Tissue Microarrays

Human tissue samples were acquired from the routine diagnostic archive of the Institute of Pathology at the University

Table 1
Overview of murine tissue samples (n = 140) from 41 transgenic mice

Genotype	No. of mice, n (%)
$KRAS^{+/-}$, $TP53^{+/+}$, $TNC^{+/+}$, $POSTN^{+/+}$ ($Ptf1aCre^{tg/+}$;$LSL\text{-}Kras^{G12D/+}$)	6 (15)
$KRAS^{+/-}$, $TP53^{-/-}$, $TNC^{+/+}$, POSTN- ($Ptf1aCre^{tg/+}$;$LSL\text{-}Kras^{G12D/+}$;$p53^{flox/flox}$)	12 (29)
$KRAS^{+/-}$, $TP53^{+/-}$, $TNC^{-/-}$, $POSTN^{+/+}$ ($Ptf1aCre^{tg/+}$;$LSL\text{-}Kras^{G12D/+}$;$p53^{flox/+}$;$TNC^{-/-}$)	4 (10)
$KRAS^{+/-}$, $TP53^{-/-}$, $TNC^{-/-}$, $POSTN^{+/+}$ ($Ptf1aCre^{tg/+}$;$LSL\text{-}Kras^{G12D/+}$;$p53^{flox/flox}$;$POSTN^{+/-}$;$TNC^{-/-}$)	9 (22)
$KRAS^{+/-}$, $TP53^{+/+}$, $TNC^{+/+}$, $POSTN^{-/-}$ ($Ptf1aCre^{tg/+}$;$LSL\text{-}Kras^{G12D/+}$;$POSTN^{-/-}$)	1 (2)
$KRAS^{+/-}$, $TP53^{+/-}$, $TNC^{+/+}$, $POSTN^{-/-}$ ($Ptf1aCre^{tg/+}$;$LSL\text{-}Kras^{G12D/+}$;$p53^{flox/+}$;$POSTN^{-/-}$)	5 (10)
$KRAS^{+/-}$, $TP53^{-/-}$, $TNC^{+/+}$, $POSTN^{-/-}$ ($Ptf1aCre^{tg/+}$;$LSL\text{-}Kras^{G12D/+}$;$p53^{flox/flox}$;$POSTN^{-/-}$)	4 (10)
140 TMA samples of	
Normal pancreatic tissue	18
ADM	21
PanIN low grade	31
PDAC (central tumor region)	35
PDAC (peripheral tumor region)	35

ADM, acinar-ductal metaplasia; IPMN, intraductal papillary mucinous neoplasm; MCN, mucinous cystic neoplasm; PanIN, pancreatic intraepithelial neoplasm; PDAC, pancreatic ductal adenocarcinoma.

Hospital of Dusseldorf, Germany. Samples include tissue from patients who underwent pancreatic surgery at the University Hospital of Dusseldorf between 2008 and 2016 (n = 76). All available hematoxylin and eosin slides were re-evaluated, and diagnoses were updated to the newest classifications and terminology.[15] In total, 221 TMA spots were created: regions of interest from normal pancreatic tissue, pancreatic cancer precursors lesions (ADM; PanIN; intraductal papillary mucinous neoplasm [IPMN]; intraductal oncocytic papillary neoplasm [IOPN]; and mucinous cystic neoplasm [MCN]), invasive PDAC and their surrounding microenvironment, respectively, were selected and transferred to TMA blocks. A 2-mm core size was used for human tissue TMAs to ensure sufficient TME was included for each lesion. Tissue cores from normal lymph nodes were included as positive controls. An overview of all human TMA samples is given in Table 2. Of note, IOPN and pancreatobiliary IPMN were not used for statistical analyses, as only 1 case per entity was available, respectively.

Multiplex Immunofluorescence for Human and Murine Tissue Samples

Multiplex immunofluorescence (mIF) allows for the simultaneous staining of a single tissue sample with multiple antibodies. Reagents from the Opal7-Color Manual IHC Kit (PerkinElmer) were used. Heat-induced epitope retrieval was achieved by incubating slides in a microwave on medium heat for 15 minutes. Endogenous peroxidase blocking and protein blocking was achieved by applying 3% H_2O_2 in phosophate-buffered saline for 20 minutes and Antibody Blocking Solution for 10 minutes. Subsequently, the first primary antibody diluted in Antibody Diluent/Blocking Solution was applied onto the slides and incubated overnight. Afterward, the secondary antibody (Opal Polymer HRP mouse and rabbit antibody) was applied for 10 minutes. Subsequently, Opal Fluorophore Working Solution (containing the respective fluorochrome und Amplification Diluent, 1:100) was applied to the slides and incubated for 10 minutes. To resolve the primary-secondary antibody complex, slides were then heated in the microwave for 15 minutes. Afterward, the protocol was repeated starting from the blocking step, using the further primary antibodies. Each of them was incubated for 60 minutes at room temperature. For each antibody, a different fluorochrome with a different wavelength spectrum was used. Finally, slides were counterstained with 4′,6-diamidino-2-phenylindole (DAPI) working solution for 5 minutes. All primary antibodies and respective fluorochromes are listed in Supplementary Table S1 (murine samples) and Supplementary Table S2 (human samples).

Table 2
Overview of human tissue samples (n = 221) from 76 patients

Characteristic	Value
Sex, n (%)	
Female	45 (59)
Male	31 (41)
Age (y), median (range)	72 (26-84)
221 TMA samples of (n)	
Normal pancreatic tissue	69
ADM	16
PanIN low grade	25
PanIN high grade	7
IPMN gastric low grade	28
IPMN gastric high grade	7
IPMN intestinal low grade	5
IPMN intestinal high grade	9
IPMN pancreatobiliary	1
IOPN	1
PDAC (central tumor region)	22
PDAC (peripheral tumor region)	22
MCN low grade	8
MCN high grade	1

ADM, acinar-ductal metaplasia; IOPN, intraductal oncocytic papillary neoplasm; IPMN, intraductal papillary mucinous neoplasm; MCN, mucinous cystic neoplasm; PanIN, pancreatic intraepithelial neoplasm; PDAC, pancreatic ductal adenocarcinoma.

p53 Immunohistochemistry of Human Tissue Samples

TMAs of human tissue samples were stained with an anti-p53 mouse monoclonal antibody (clone DO-1) at a dilution of 1:200 on the BenchMark automated IHC/ISH slide staining system (Ventana Medical Systems) according to the protocol established for routine diagnostics at the Institute of Pathology at the University Hospital of Dusseldorf, Germany. Aberrant p53 staining was defined as either overexpression (strong nuclear staining in $\geq$80% of nuclei) or total loss of staining. Cells in surrounding stroma served as internal control.

Image Data Processing and Semiautomated Image Analysis

mIF was visualized using a Leica TCS SP8 STED 3× confocal microscope equipped with a HC PL APO CS2 20×/0.75 multiimmersion objective (Leica Microsystems). Images were taken using Leica Application Suite X software (Leica Microsystems). Further image analysis was performed with FIJI/ImageJ (National Institutes of Health). To account for differences in staining intensities and background staining between different antibodies, an individual macro was written for the semiautomated analysis of each antibody in each tissue type (murine vs human). Macros defined parameters for thresholding, smoothing, and determining the minimum and maximum size of the stained particles to be counted. In brief, macros thresholded the channel of choice using the Yen-autothreshold algorithm and removed single pixel events in the first place by the despecle function. Positive areas were counted by the analyze particle function, and detailed readout results (number and area) were used for downstream analysis. An exemplary FIJI macro (used for FoxP3 analysis) and exemplary input and result data are provided at https://github.com/SHaensch/2025_FoxP3Quant. For each sample and marker, the total number of cells stained with the respective antibody was counted. Subsequently, marker-positive cell counts and total cell counts (DAPI-positive cells) were first normalized to tissue area (cells/mm^2). Their ratio was then calculated (marker-positive cells/area in mm^2 divided by DAPI-positive cells/area in mm^2), yielding the proportion of marker-positive cells in percentage, independent of tissue area.

Statistical Analysis

Statistical analyses were performed using SPSS (version 29; SPSS Inc., Chicago, IL, USA). Kruskal–Wallis test was used to compare median values of >2 groups. Dunn–Bonferroni correction was used during post hoc analysis. *P* value of <.05 was considered statistically significant. Graphs in Figures 1 to 4 were created using GraphPad Prism (version 1.3.1; GraphPad Software Inc., Boston, MA, USA).

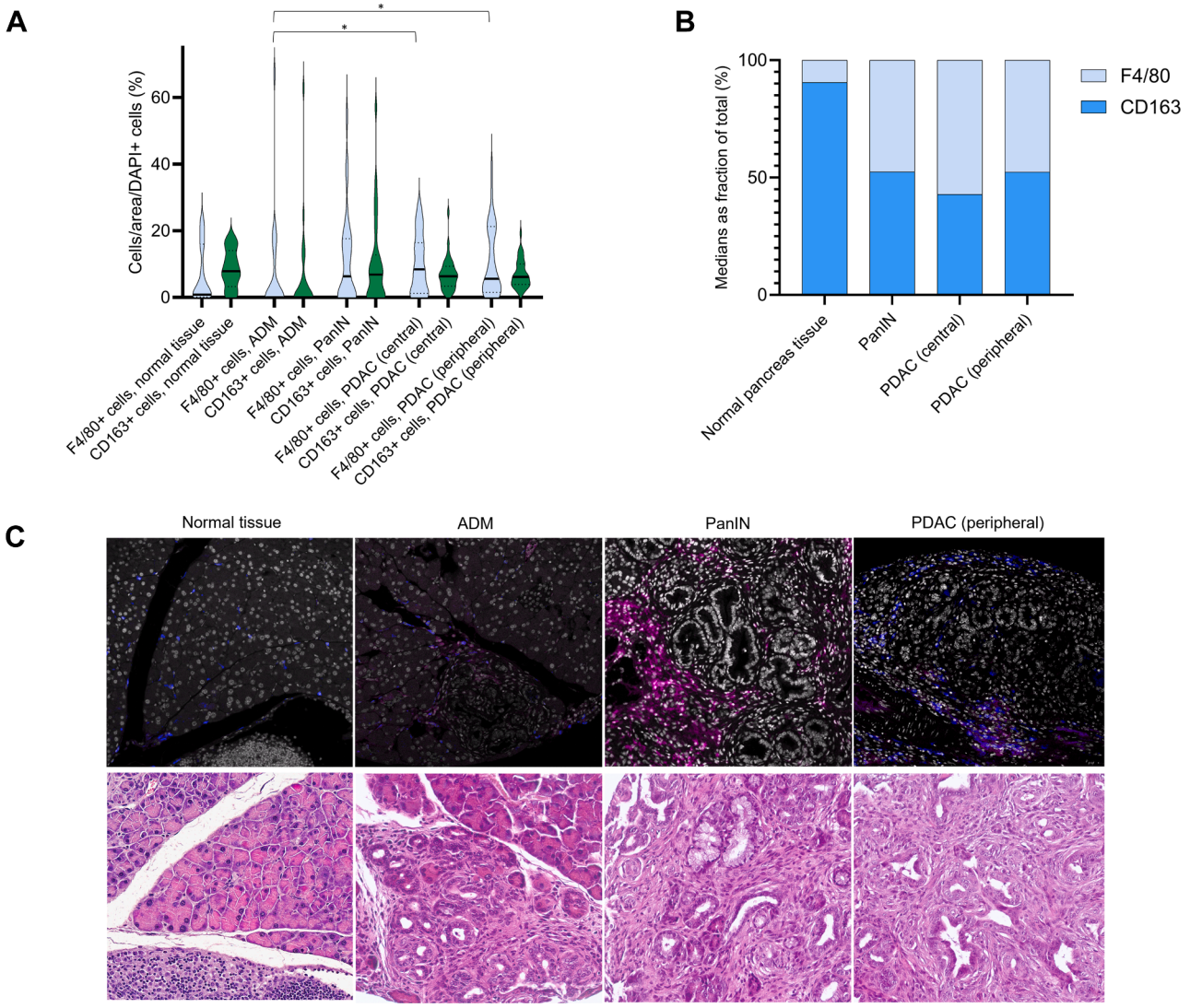

Figure 1.
Innate immune response in pancreatic ductal adenocarcinoma (PDAC) mouse models. (A) F4/80$^+$ macrophages (light blue plots) are increased in PDAC compared with acinar-ductal metaplasia (ADM). No statistically significant differences in the relative numbers of CD163$^+$ (M2) macrophages (green plots) alone are noted when comparing PDAC, precursors, and normal pancreas tissue. *$P < .05$. (B) Large proportions of the F4/80$^+$ macrophages are also CD163$^+$, indicating M2 macrophages (dark blue columns). (C) Macrophages are increased in pancreatic intraepithelial neoplasm (PanIN) and PDAC compared with normal pancreas and ADM. Pink, F4/80$^+$ macrophages; blue, CD163$^+$ M2 macrophages; gray, 4′,6-diamidino-2-phenylindole (DAPI; magnification, ×200). Second row: corresponding hematoxylin and eosin stainings.

Results

Innate Immune Response in Mouse Models of Pancreatic Ductal Adenocarcinoma and Its Precursors

Supplementary Table S3 presents the median values and ranges (minimum to maximum) of immune cells positive for each marker across all evaluated murine tissue types. Values are given as percentages of all DAPI-positive cells. In mice, tryptase-positive mast cells were significantly enriched in PDAC (central PDAC: 24.31%; $P = .008$; peripheral PDAC: 31.98%; $P = .001$), compared with those in normal pancreatic tissue (11.47%).

Similarly, F4/80$^+$ macrophages were increased in PDAC (central PDAC: 8.43%; $P = .029$; peripheral PDAC: 5.59%; $P = .012$) compared with those in ADM (median: 0.00%) (Fig. 1A). It was noted that a large proportion of the F4/80$^+$ macrophages were CD163$^+$ M2 macrophages (Fig. 1B, C). However, a comparison of the relative numbers of CD163$^+$ cells alone in PDAC vs precursors vs normal pancreas tissue yielded no statistically significant differences (Fig. 1A). The numbers of mast cells and macrophages were not significantly increased in murine precursors (ADM or PanIN) when comparing them with normal murine pancreas tissue.

Innate Immune Response in Human Pancreatic Ductal Adenocarcinoma and Its Precursors

Supplementary Tables S4 and S5 show the median values and ranges (minimum to maximum) of immune cells positive for each marker across all evaluated human tissue types. Values are given as percentages of all DAPI-positive cells.

In human tissue samples, tryptase-positive mast cells were increased in several precursor lesions compared with those in normal tissue. The median percentage of tryptase-positive cells in normal tissue was 1.12%; in ADM, 3.78% ($P < .001$ vs normal); in PanIN, 3.00% ($P < .001$); in gastric IPMN, 3.13% ($P < .001$); and in

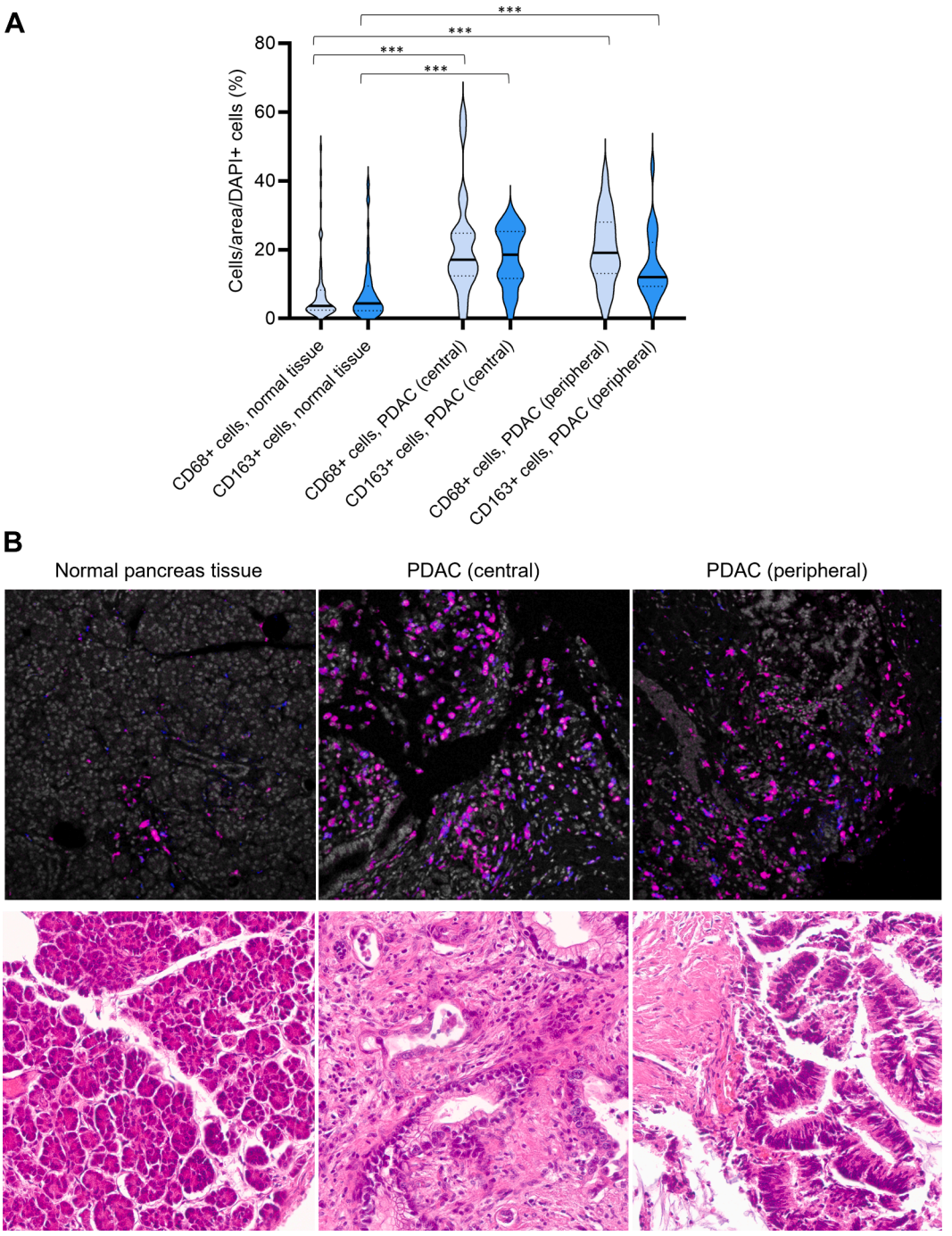

Figure 2.
Macrophages in human pancreatic ductal adenocarcinoma (PDAC). (A) All macrophages ($CD68^+$ cells, light blue plots) and M2 macrophages ($CD163^+$ cells, dark blue plots) are significantly enriched in human PDAC compared with normal pancreatic tissue. ***$P < .001$. (B) Multiplex immunofluorescence shows an increase in $CD68^+$ and $CD163^+$ cells in PDAC compared with those in normal pancreas tissue. Pink, $CD68^+$ macrophages; blue, $CD163^+$ M2 macrophages; gray, DAPI (magnification, ×200). Second row, corresponding hematoxylin and eosin stainings.

intestinal IPMN, 2.34% ($P = .021$). However, in PDAC, mast cell numbers decreased again to levels similar to those in normal tissue (1.77%; no statistically significant difference compared with normal tissue), indicating a dynamic immunomodulatory process.

Macrophages (identified via CD68 positivity in human samples) were increased in human ADM and PDAC compared with normal tissue. The median percentage of $CD68^+$ cells was 3.70% in normal pancreas tissue, whereas it was 22.16% in ADM ($P < .001$) and 17.57% in PDAC ($P < .001$).

Contrary to results in mice, we could also demonstrate a significant increase of $CD163^+$ M2 macrophages in human ADM and PDAC tissue samples: The median percentage of $CD163^+$ cells was 4.39% in normal pancreatic tissue, but 12.59% in ADM ($P = .008$), 18.57% in central PDAC ($P < .001$), and 12.02% in peripheral PDAC ($P < .001$) (Fig. 2).

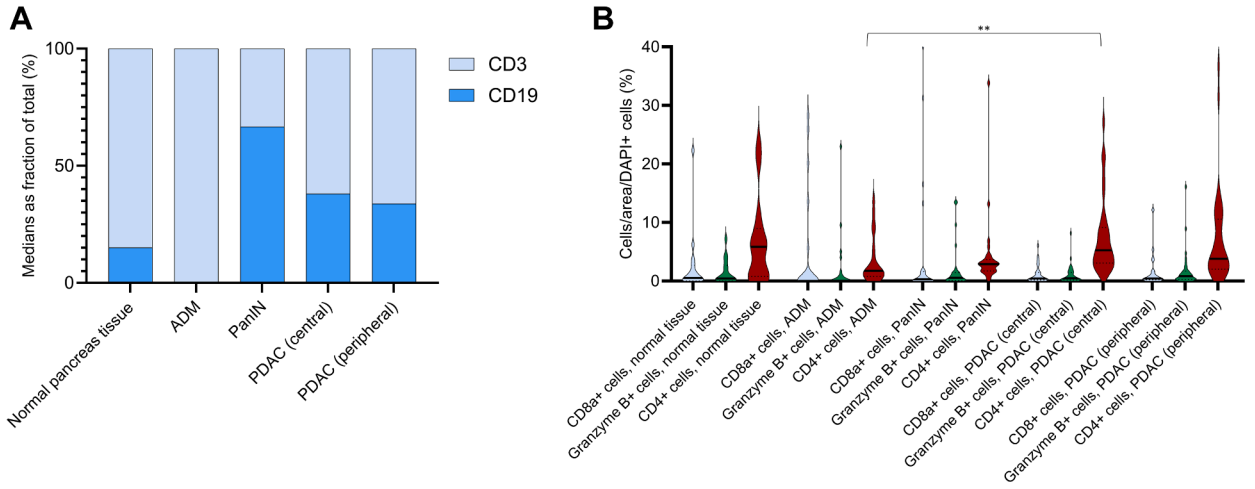

Figure 3.
Adaptive immune response in pancreatic ductal adenocarcinoma (PDAC) mouse models. A. Most lymphocytes in murine normal pancreas tissue, acinar-ductal metaplasia (ADM), and PDAC are CD3$^+$ T cells (light blue columns), whereas CD19$^+$ B cells (dark blue columns) dominate only in PanIN. (B) CD4$^+$ T helper cells (dark red plots) are the most common type of T cells in murine tissue and show a significant increase in central PDAC tissue compared with ADM tissue. $^{**}P < 0.01$. No significant differences can be noted regarding the fraction of CD8a$^+$/granzyme B$^+$ T cells between PDAC vs precursors vs normal pancreas tissue in mice.

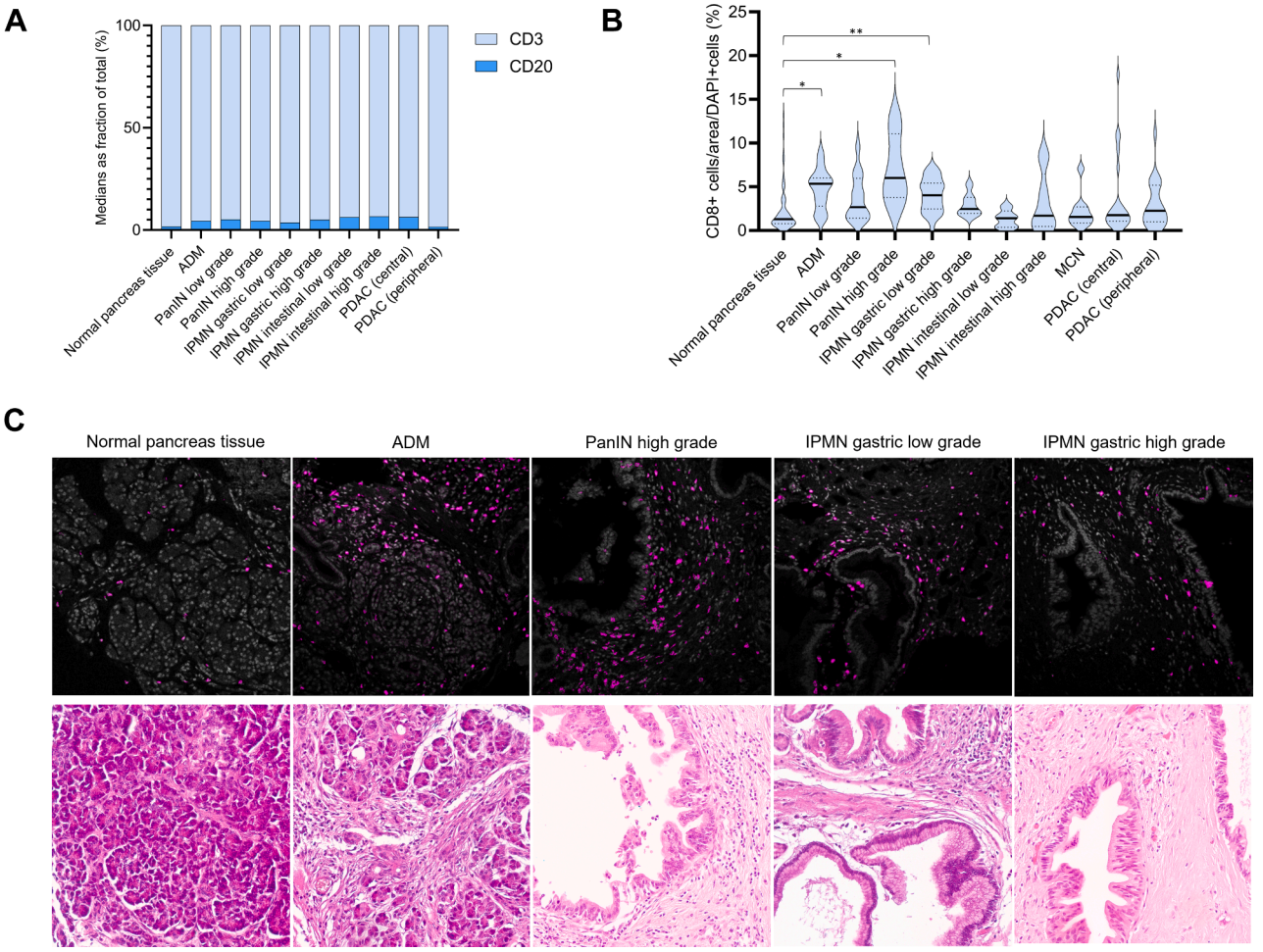

Figure 4.
Adaptive immune response in human pancreatic ductal adenocarcinoma (PDAC) and its precursors. (A) Adaptive immune response in human pancreatic carcinogenesis is consistently dominated by CD3$^+$ T lymphocytes (light blue columns) rather than CD20$^+$ B lymphocytes (dark blue columns). (B) The number of CD8$^+$ cytotoxic T cells is highly dynamic in human pancreatic carcinogenesis, showing an increase in some precursor lesions (ADM, PanIN high grade, and intraductal papillary mucinous neoplasm [IPMN] gastric low grade), but low numbers of CD8$^+$ T cells in intestinal IPMN, mucinous cystic neoplasm (MCN), and invasive PDAC. $^*P < .05$; $^{**}P < .01$. (C) Compared with normal pancreas tissue, CD8$^+$ cytotoxic T cells are increased in ADM, high-grade PanIN, and low-grade gastric IPMN, whereas high-grade gastric IPMN show a slight decrease in CD8$^+$ cells. Pink, CD8$^+$ cytotoxic T cells; gray, DAPI (magnification, ×200). Second row, corresponding hematoxylin and eosin stainings.

Of note, both CD68$^+$ and CD163$^+$ (M2) macrophages showed a broad range of abundance in human PDAC precursor lesions, including earlier precursors such as ADM (CD68$^+$ cells: range, 5.73%-41.75%; CD163$^+$ cells: range, 2.60%-36.20%), as well as high-grade precursors, such as intestinal IPMN high-grade (CD68$^+$ cells: range, 2.59%-38.78%; CD163$^+$ cells: range, 1.06%-18.18%).

Adaptive Immune Response in Mouse Models of Pancreatic Ductal Adenocarcinoma and Its Precursors

Comparison of CD3$^+$ T cells and CD19$^+$ B cells in murine tissues showed a relative predominance of T lymphocytes over B lymphocytes in the immune infiltrate of central and peripheral PDAC, ADM, and normal pancreatic tissue. In contrast, a relative predominance of B cells was found only in PanIN (Fig. 3A).

The most prevalent T cell type in all murine tissues were CD4$^+$ T helper cells. T helper cells were not only higher in relative numbers than in CD8$^+$/granzyme B$^+$ cytotoxic T cells in murine PDAC, precursors, and normal pancreas tissue but also showed a statistically significant increase when comparing central PDAC (5.25%) with ADM (1.74%; $P = .008$) (Fig. 3B).

FoxP3$^+$ regulatory T cells represented only a small proportion of all CD4$^+$ T cells in all murine tissues (medians, <0.5% across all murine tissue types). Proportions of PD-1$^+$ immune cells ranged from 0% to 30.67% in murine tissue types (median, 1.89%). Murine ADM, PanIN, and PDAC showed slightly increased numbers of PD-1$^+$ immune cells compared with murine normal pancreas tissue; however, differences were not statistically significant.

Influence of Mouse Genotype on Immune Microenvironment

Tissues of mice with *Tp53* wild-type (n = 7) showed significantly higher numbers of CD3$^+$ T cells than heterozygous *Tp53* knockout mice (n = 9) and homozygous *Tp53* knockout mice (n = 25; both $P < .05$), which could suggest effects on the iME as a facilitating factor within the prognostically unfavorable role of *Tp53* mutations in human PDAC. Additional knockouts of the ECM protein TNC or POSTN had no observable effect on the immune cell infiltrate of murine PDAC or precursor lesions.

Adaptive Immune Response in Human Pancreatic Ductal Adenocarcinoma and Its Precursors

Pancreatic normal tissue, all analyzed pancreatic precursors lesions (ADM, PanIN, IPMN, IOPN, and MCN), and PDAC showed a strong predominance of CD3$^+$ T lymphocytes vs CD20$^+$ B lymphocytes (Fig. 4A). Notably, PanIN low grade, which showed a predominance of B cells in mouse models, showed no such exception in human tissue samples.

CD4$^+$ T cells (accounting mainly for T helper cells) showed increased numbers in ADM (4.15%; $P = .004$), PanIN (3.16%; $P = .008$), gastric-type IPMN (2.91%; $P = .048$), and PDAC (4.85%; $P < .001$), compared with normal pancreas tissue (1.22%). Similarly, FoxP3+ Tregs were increased in human ADM (0.11%; $P = .003$), PanIN (0.07%; $P = .043$), gastric-type IPMN (0.08%; $P = .003$), and PDAC (0.15%; $P < .001$), when compared with normal tissue (0.02%). No significant differences in T helper cell or Treg numbers could be noted in other pancreatic cancer precursors vs normal tissue.

Although CD8$^+$ cytotoxic T cells showed generally low levels in murine tissues and no significant differences between murine pancreatic tissue types (PDAC vs precursors vs normal pancreas tissue), significant differences were observed in human tissue samples. In human samples, normal tissue showed low levels of cytotoxic T cells (median 1.31%), whereas CD8$^+$ cells were enriched in ADM (5.34%; $P = .007$), PanIN (3.94%; $P = .002$), and gastric-type IPMN (3.73%; $P = .001$) but not in other precursor lesions such as intestinal-type IPMN or MCN (Fig. 4B, C). PDAC tissue showed low numbers of CD8$^+$ cytotoxic T cells (1.93%; no statistically significant difference to pancreatic normal tissue), congruent with its known immunosuppressive microenvironment (Fig. 4B, C).

PD-1$^+$ immune cells were generally sparse in human tissue types. However, a significant increase of PD-1$^+$ immune cells could be noted comparing human ADM (0.04%; $P = .043$), PanIN (0.05%; $P = .006$), gastric-type IPMN (0.06%; $P < .001$), and PDAC (0.02%; $P = .029$) with normal human pancreas tissue (median, 0.00%).

Association between p53 Status and Immune Microenvironment in Human Tissue Samples

In TMAs containing human tissue samples, lesions displaying a p53 wild-type staining pattern were compared with lesions showing aberrant p53 staining with respect to abundance of CD3$^+$ cells; in human tissue samples, no significant differences were observed (not shown).

Discussion

Immune Microenvironment in Human PDAC and Its Precursors

The iME is characterized by a heterogeneous and highly dynamic pattern during pancreatic carcinogenesis. Relevant effects of the pancreatic cancer iME on the course of disease have been described in the literature. For example, it has recently been shown that nonrecurrent pancreatic cancer is characterized by an active response of the adaptive immune system and is rich in proinflammatory cytokines.[16]

In this study, a synchronous analysis of murine and human tissues using identical methodology was undertaken to achieve a detailed and comparative characterization of iME of various precursors in both mouse models and human tissue samples. The cohorts used in this study consist of PDAC, PDAC precursors, and normal pancreatic tissue. All lesions were (re-)characterized according to the newest classification system to ensure reliable and reproducible results.

Notably, we were able to show that changes in the iME occur as early as in the state of metaplasia, namely during ADM. Interestingly, human ADM already seem to be enriched in cell types typically associated with immunosuppression, such as CD163$^+$ M2 macrophages, CD4$^+$ T helper cells, and FoxP3$^+$ Tregs. Although human PanIN and gastric IPMN very similarly showed an increase in T helper cells and Tregs, intestinal IPMN and MCN did not show a significant increase in these cell types. Transcriptome studies have delivered evidence that even early PDAC precursor lesions such as ADM and PanIN may in fact have the potential to recruit and interact with immune cells.[17]

On the contrary, cytotoxic T cells, which are typically thought of as immunoactive cells, seem to show very variable levels in human pancreatic tissues during carcinogenesis. Cytotoxic T cells were significantly elevated in ADM and other pancreatic cancer

precursor lesions but seem to decrease again in PDAC, compatible with the known immunosuppressive microenvironment of PDAC. The immunosuppressive nature of PDAC iME is further corroborated by the fact that immunosuppressive cells were shown to be enriched in PDAC ($CD4^+$ T helper cells, $FoxP3^+$ Tregs, and $CD163^+$ M2 macrophages) in this study.

Regarding the cytotoxic T cell response, it is very notable that some precursors—namely, ADM, PanIN, and gastric IPMN—seem to show a transient increase in T cell response during carcinogenesis, whereas others—such as intestinal IPMN and MCN—do not. This seems to be in line with results of extensive (epi-)genetic studies, which underscored the close similarities between PanIN and gastric IPMN and significant differences between those lesions on one hand and intestinal IPMN on the other hand, which may be linked to different cells of origin and different patterns of injury triggering their development.[18] Because many studies have focused on IPMN as a single entity with no separate analyses of different histotypes, extensive data are yet missing. As most gastric-type IPMN are low-grade IPMN and most intestinal-type IPMN are high-grade IPMN—a distribution that is also reflected in the samples used in this study (Table 2)—, it is also possible that IPMN show cytotoxic T cell response in earlier stages and lose it during progression to high-grade lesions. Recently published studies also identify the critical turning point in the progression model of IPMN at the transition from low-grade to high-grade dysplasia, demonstrating a significant increase of macrophages and decrease of cytotoxic T cells at this step.[19,20] It was pointed out in a recent study that increasing numbers of macrophages in human IPMN were often restricted to focal regions of high-grade dysplasia,[19] which may explain broad ranges in macrophage abundance across different cases from the same lesion types found in our study and could be resulting from the fact that macrophages are niche-dependent cells responding to local microenvironmental cues. However, it must be noted that larger areas within single lesions were not evaluated in the present study, as TMAs were used. Findings underscoring the global decrease of cytotoxic T cells during the shift from low-grade to high-grade lesions[19] have led to the suggestion that the progression of low-grade IPMN could possibly be delayed by therapies supporting the cytotoxic T cell reaction.[21] As the immunosuppression in IPMN in particular seems to be mediated by PD-L1 expression on immune cells, immunotherapeutic strategies using anti–PD-1 substances may reverse the associated immunosuppression in high-risk IPMN.[22] The lack of a prominent T cell response in MCN, on the contrary, could possibly be explained by the fact that their development and growth is hormone-dependent rather than immune-dependent. Other studies have also shown that the increase of $CD8^+$ T cells is significantly higher in IPMN than those in MCN when compared with normal pancreas tissue.[23]

Another level of complexity is introduced by recent 3-dimensional morphomolecular analyses of pancreatic precursors, largely focused on PanIN. These studies indicate that these lesions are frequent, spatially extensive, and clonally heterogeneous, with true 3-dimensional size often exceeding what is appreciated in 2-dimensional sections, challenging the traditional size-based classification scheme.[24,25] In fact, there are findings suggesting that the iME of PanIN, in particular, seems to be not only heterogeneous but also depending on the level of dysplasia and size.[26] Such heterogeneity at the precursor level implies that epithelial evolution occurs within a nonuniform tissue context, prompting the question of how local iMEs differ across precursor lesions and whether immune composition or spatial organization contributes to lesion fate.

Immune Microenvironment in Mouse Models of PDAC and Its Precursors

Although transgenic mouse models do show a similar immunosuppressive iME in PDAC as in human PDAC (rich in macrophages and T helper cells), results regarding the iME of precursors—namely ADM and PanIN—differ from those found in human tissues in the presented study. Notably, neither murine ADM nor murine PanIN showed any significant increase in $CD8^+$ cytotoxic T cells. This suggests that caution must be taken when translating findings from mouse models to humans regarding iME during pancreatic carcinogenesis. Of note, murine PanIN also represent the only precursor lesion within this study in which B cells generally predominated over T cells. Depending on their subtype, B cells can either play an immunoactive role (eg, presenting tumor antigens to T cells and producing antitumoral antibodies) or an immunosuppressive role (eg, regulatory B cells producing anti-inflammatory cytokines) in pancreatic carcinogenesis.[27-29] Similar to our results, a study using a KPC mouse model also found an unexpectedly high number of $CD19^+$ B cells in KPC mouse samples, including PanIN of KPC mice.[30] A classification of B cell subtypes is needed in the future to further elucidate the role (immunoactive vs immunosuppressive) of B cells in pancreatic iME.

We found a significant influence of *Tp53* mutational status on the infiltration of murine tissues with cells of the adaptive immune system. In comparison with *Tp53* wild-type mice, we found significantly lower numbers of T cells in *Tp53* knockout mice. This may be due to the ability of the tumor suppressor p53 to communicate with the adaptive immune system and influence the cytotoxic T cell response, possibly by regulating the expression of major histocompatibility complex I (MHC I) on the cell surface.[31-33] Whether a similar effect is in place during human pancreatic carcinogenesis is yet to be elucidated; however, it is known that an active cytotoxic T cell response is linked to favorable prognosis in human PDAC, on one hand,[3,16] and that *TP53* mutations are linked to poorer prognosis in human PDAC, on the other hand.[34]

Elusive Effect of TNC and POSTN on the Immune Microenvironment of Pancreatic Cancer and Its Precursors

Transgenic mice with an additional knockout of the ECM proteins TNC and POSTN, respectively, were included in this study to evaluate the influence of both proteins on pancreatic carcinogenesis. Although both have been shown to exert immunomodulatory functions,[12-14] no effect of TNC or POSTN could be demonstrated in this study. Although this study provides a detailed quantitative analysis of the iME in a thoroughly characterized cohort, some qualitative changes in immune cells may remain undetected. For example, a main mechanism of immunosuppression of TNC studied in the literature is the entrapment of $CD8^+$ cytotoxic T cells.[12,13] This does not necessarily equal a change in $CD8^+$ cytotoxic T cell numbers, and a detailed spatial analysis of the tissue may be needed to verify this effect. Similarly, proinflammatory effects of TNC exerted by upregulation of genes related to antigen processing and presentation within immune cells may evade detection by our quantitative-centered approach. Although POSTN has been suggested to affect the number of infiltrating M2 macrophages,[14] this cell type was generally rare within murine tissue (Fig. 1A). Thus, changes may have been too subtle to detect using only mIF. In general, methods offering high-resolution insights into the iME, such as single-cell RNA sequencing or spatial transcriptomics, may be needed to

unveil TNC- and POSTN-related functional changes—for example, in gene expression profiles or cytokine production—, to study rare cell types, and to uncover possible compensatory mechanisms, that is, the upregulation of other proteins linked to TNC/POSTN knockout.

In conclusion, this study focused on the temporal evolution of iME in murine and human pancreatic carcinogenesis and on the differences of iME in different precursor lesions. We could show that certain immune cell populations in early precursors show changes comparable in magnitude with those in invasive PDAC. This aligns with the emerging concept that pancreatic precursor lesions are biologically active and induce stromal remodeling and immune cell engagement well before overt invasion.[35] Mechanistically, immune cell alterations in preinvasive lesions can be explained by tissue injury associated with chronic inflammation and effects of early genetic events such as *KRAS* mutations.[36]

Further studies are needed to gain a deeper understanding of the spatial relationship between pancreatic cancer precursors and iME—for example, distinguishing loose vs dense immune cell infiltration or intratumoral vs peritumoral immune cell infiltrates—and to verify the functional relevance of quantitative changes. Although the present study focused on the most common PDAC precursors, rare precursor subtypes with high malignant potential, such as IOPN and pancreatobiliary-type IPMN, represent distinct entities with potentially unique immune microenvironmental features and will require dedicated future studies.

Acknowledgments

The authors gratefully acknowledge the support of all members of Esposito's laboratory at the Institute of Pathology, University Hospital of Duesseldorf.

Author Contributions

I.E performed study concept and design. I.E., L.H.-G., M. Schulte, C.M., and M. Schlensog performed development of methodology and writing, review and revision of the paper. M. Schulte, C.M., L.H., S.H., M. Schlensog, and I.E. provided acquisition, analysis and interpretation of data, and statistical analysis. All authors approved of the final version of the manuscript.

Data Availability

The data supporting the findings of this study are available from the corresponding author upon reasonable request. Human data can only be provided in pseudonymized form in compliance with data protection regulations and institutional ethics approval.

Funding

This study was supported by internal funding from Heinrich Heine University Duesseldorf (Duesseldorf School of Oncology), in the form of a doctoral scholarship for medical students awarded to coauthor Marie Schulte.

Declaration of Competing Interest

The authors declare no competing interest.

Ethics Approval and Consent to Participate

The study was conducted in accordance with the Declaration of Helsinki. The use of human tissue samples was approved by the local ethics committee at the Medical Faculty of the Heinrich Heine University of Duesseldorf (ethic vote no. 2022-2170). Written informed consent was waived by the ethics committee due to the retrospective nature of this study and use of pseudonymized data. All animal experiments were carried out in accordance with the ARRIVE guidelines and the EU Directive 2010/63/EU for animal experiments. Animal necropsies and organ examination were approved by the North Rhine-Westphalian Office of Nature, Environment and Consumer Protection (LANUV NRW) (Animal testing application No. 84-02.04.2016A060).

Declaration of Generative AI and AI-Assisted Technologies in the Writing Process

During the preparation of this work, the authors used ChatGPT (OpenAI) in order to refine the language in the article. No content generation or data interpretation was performed using AI. After using this tool, the authors reviewed and edited the content as needed and take full responsibility for the content of the published article.

Supplementary Material

The online version contains supplementary material available at https://doi.org/10.1016/j.labinv.2026.106143

References

1. Cronin KA, Scott S, Firth AU, et al. Annual report to the nation on the status of cancer, part 1: national cancer statistics. *Cancer*. 2022;128(24):4251–4284. https://doi.org/10.1002/cncr.34479
2. Vogelstein B, Papadopoulos N, Velculescu VE, Zhou S, Diaz LA Jr, Kinzler KW. Cancer genome landscapes. *Science*. 2013;339(6127):1546–1558. https://doi.org/10.1126/science.1235122
3. Balachandran VP, Łuksza M, Zhao JN, et al. Identification of unique neoantigen qualities in long-term survivors of pancreatic cancer. *Nature*. 2017;551(7681):512–516. https://doi.org/10.1038/nature24462
4. Le DT, Durham JN, Smith KN, et al. Mismatch repair deficiency predicts response of solid tumors to PD-1 blockade. *Science*. 2017;357(6349):409–413. https://doi.org/10.1126/science.aan6733
5. Luchini C, Brosens LAA, Wood LD, et al. Comprehensive characterisation of pancreatic ductal adenocarcinoma with microsatellite instability: histology, molecular pathology and clinical implications. *Gut*. 2021;70(1):148–156. https://doi.org/10.1136/gutjnl-2020-320726
6. Marabelle A, Le DT, Ascierto PA, et al. Efficacy of pembrolizumab in patients with noncolorectal high microsatellite instability/mismatch repair-deficient cancer: results from the phase II KEYNOTE-158 study. *J Clin Oncol*. 2020;38(1):1–10. https://doi.org/10.1200/jco.19.02105
7. Mittal D, Gubin MM, Schreiber RD, Smyth MJ. New insights into cancer immunoediting and its three component phases—elimination, equilibrium and escape. *Curr Opin Immunol*. 2014;27:16–25. https://doi.org/10.1016/j.coi.2014.01.004
8. Lu C, Paschall AV, Shi H, et al. The MLL1-H3K4me3 axis-mediated PD-L1 expression and pancreatic cancer immune evasion. *J Natl Cancer Inst*. 2017;109(6):djw283. https://doi.org/10.1093/jnci/djw283
9. Esposito I, Penzel R, Chaib-Harrireche M, et al. Tenascin C and annexin II expression in the process of pancreatic carcinogenesis. *J Pathol*. 2006;208(5):673–685. https://doi.org/10.1002/path.1935
10. Paron I, Berchtold S, Vörös J, et al. Tenascin-C enhances pancreatic cancer cell growth and motility and affects cell adhesion through activation of the integrin pathway. *PLoS One*. 2011;6(6):e21684. https://doi.org/10.1371/journal.pone.0021684
11. Erkan M, Kleeff J, Gorbachevski A, et al. Periostin creates a tumor-supportive microenvironment in the pancreas by sustaining fibrogenic stellate cell activity. *Gastroenterology*. 2007;132(4):1447–1464. https://doi.org/10.1053/j.gastro.2007.01.031

12. Dhaouadi S, Bouhaouala-Zahar B, Orend G. Tenascin-C targeting strategies in cancer. *Matrix Biol*. 2024;130:1–19. https://doi.org/10.1016/j.matbio.2024.04.002
13. Yilmaz A, Loustau T, Salomé N, et al. Advances on the roles of tenascin-C in cancer. *J Cell Sci*. 2022;135(18):jcs260244. https://doi.org/10.1242/jcs.260244
14. Chen Y, Zhang F, Zhang B, et al. Periostin is associated with prognosis and immune cell infiltration in pancreatic adenocarcinoma based on integrated bioinformatics analysis. *Cancer Rep (Hoboken)*. 2024;7(2):e1990. https://doi.org/10.1002/cnr2.1990
15. WHO Classification of Tumours Editorial Board. *Digestive System Tumours. WHO Classification of Tumours, 5th Edition, Volume 1*. Lyon, France: International Agency for Research on Cancer (IARC); 2019.
16. Karamitopoulou E, Wenning AS, Acharjee A, et al. Spatially restricted tumour-associated and host-associated immune drivers correlate with the recurrence sites of pancreatic cancer. *Gut*. 2023;72(8):1523–1533. https://doi.org/10.1136/gutjnl-2022-329371
17. Schlesinger Y, Yosefov-Levi O, Kolodkin-Gal D, et al. Single-cell transcriptomes of pancreatic preinvasive lesions and cancer reveal acinar metaplastic cells' heterogeneity. *Nat Commun*. 2020;11(1):4516. https://doi.org/10.1038/s41467-020-18207-z
18. Liffers ST, Godfrey L, Frohn L, et al. Molecular heterogeneity and commonalities in pancreatic cancer precursors with gastric and intestinal phenotype. *Gut*. 2023;72(3):522–534. https://doi.org/10.1136/gutjnl-2021-326550
19. Jamouss KT, Damanakis AI, Cornwell AC, et al. Tumor immune microenvironment alterations associated with progression in human intraductal papillary mucinous neoplasms. *J Pathol*. 2025;266(1):40–50. https://doi.org/10.1002/path.6402
20. Eckhoff AM, Fletcher AA, Landa K, et al. Multidimensional immunophenotyping of intraductal papillary mucinous neoplasms reveals novel T Cell and macrophage signature. *Ann Surg Oncol*. Nov 2022;29(12):7781–7788. https://doi.org/10.1245/s10434-022-12157-0
21. Pollini T, Adsay V, Capurso G, et al. The tumour immune microenvironment and microbiome of pancreatic intraductal papillary mucinous neoplasms. *Lancet Gastroenterol Hepatol*. 2022;7(12):1141–1150. https://doi.org/10.1016/s2468-1253(22)00235-7
22. Enzler T, Frankel TL. Pancreatic cancer precursor lesions—can immunotherapy prevent progression into pancreatic ductal adenocarcinoma? *Cancer Lett*. 2025;619:217662. https://doi.org/10.1016/j.canlet.2025.217662
23. Enzler T, Shi J, McGue J, et al. A comparison of spatial and phenotypic immune profiles of pancreatic ductal adenocarcinoma and its precursor lesions. *Int J Mol Sci*. 2024;25(5):2953. https://doi.org/10.3390/ijms25052953
24. Braxton AM, Kiemen AL, Grahn MP, et al. 3D genomic mapping reveals multifocality of human pancreatic precancers. *Nature*. 2024;629(8012):679–687. https://doi.org/10.1038/s41586-024-07359-3
25. Kiemen AL, Dequiedt L, Shen Y, et al. PanIN or IPMN? Redefining lesion size in 3 dimensions. *Am J Surg Pathol*. 2024;48(7):839–845. https://doi.org/10.1097/pas.0000000000002245
26. Kiemen AL, Almagro-Pérez C, Matos V, et al. 3D histology reveals that immune response to pancreatic precancers is heterogeneous and depends on global pancreas structure. Preprint *bioRxiv*. Posted online August 6, 2024:606493. https://doi.org/10.1101/2024.08.03.606493
27. Spear S, Candido JB, McDermott JR, et al. Discrepancies in the tumor microenvironment of spontaneous and orthotopic murine models of pancreatic cancer uncover a new immunostimulatory phenotype for B cells. *Front Immunol*. 2019;10:542. https://doi.org/10.3389/fimmu.2019.00542
28. Gunderson AJ, Kaneda MM, Tsujikawa T, et al. Bruton tyrosine kinase-dependent immune cell cross-talk drives pancreas cancer. *Cancer Discov*. 2016;6(3):270–285. https://doi.org/10.1158/2159-8290.Cd-15-0827
29. Joseph AM, Al Aiyan A, Al-Ramadi B, Singh SK, Kishore U. Innate and adaptive immune-directed tumour microenvironment in pancreatic ductal adenocarcinoma. *Front Immunol*. 2024;15:1323198. https://doi.org/10.3389/fimmu.2024.1323198
30. Yang J, Zhang Q, Wang J, et al. Dynamic profiling of immune microenvironment during pancreatic cancer development suggests early intervention and combination strategy of immunotherapy. *EBioMedicine*. 2022;78:103958. https://doi.org/10.1016/j.ebiom.2022.103958
31. Braun MW, Iwakuma T. Regulation of cytotoxic T-cell responses by p53 in cancer. *Transl Cancer Res*. 2016;5(6):692–697. https://doi.org/10.21037/tcr.2016.11.76
32. Wang B, Niu D, Lai L, Ren EC. p53 increases MHC class I expression by upregulating the endoplasmic reticulum aminopeptidase ERAP1. *Nat Commun*. 2013;4:2359. https://doi.org/10.1038/ncomms3359
33. Zhu K, Wang J, Zhu J, Jiang J, Shou J, Chen X. p53 induces TAP1 and enhances the transport of MHC class I peptides. *Oncogene*. 1999;18(54):7740–7747. https://doi.org/10.1038/sj.onc.1203235
34. Safi SA, Haeberle L, Goering W, et al. Genetic alterations predict long-term survival in ductal adenocarcinoma of the pancreatic head. *Cancers (Basel)*. 2022;14(3):850. https://doi.org/10.3390/cancers14030850
35. Opitz FV, Haeberle L, Daum A, Esposito I. Tumor microenvironment in pancreatic intraepithelial neoplasia. *Cancers (Basel)*. 2021;13(24):6188. https://doi.org/10.3390/cancers13246188
36. Liou GY, Döppler H, Necela B, et al. Mutant KRAS-induced expression of ICAM-1 in pancreatic acinar cells causes attraction of macrophages to expedite the formation of precancerous lesions. *Cancer Discov*. 2015;5(1):52–63. https://doi.org/10.1158/2159-8290.Cd-14-0474